Action Potential Conduction Between a Ventricular Cell Model and an Isolated Ventricular Cell

Ronald Wilders,*,‡ Rajiv Kumar,§ Ronald W. Joyner,§ Habo J. Jongsma,* E. Etienne Verheijck,*,‡ David Golod,§ Antoni C. G. van Ginneken,‡ and William N. Goolsby§

*Department of Medical Physiology and Sports Medicine, Utrecht University, 3584 CG Utrecht, The Netherlands, ‡Department of Physiology, University of Amsterdam, 1105 AZ Amsterdam, The Netherlands, §Todd Franklin Cardiac Research Laboratory, The Children's Heart Center, Department of Pediatrics, Emory University, Atlanta, Georgia, USA

ABSTRACT We used the Luo and Rudy (LR) mathematical model of the guinea pig ventricular cell coupled to experimentally recorded guinea pig ventricular cells to investigate the effects of geometrical asymmetry on action potential propagation. The overall correspondence of the LR cell model with the recorded real cell action potentials was quite good, and the strength-duration curves for the real cells and for the LR model cell were in general correspondence. The experimental protocol allowed us to modify the effective size of either the simulation model or the real cell. 1) When we normalized real cell size to LR model cell size, required conductance for propagation between model cell and real cell was greater than that found for conduction between two LR model cells (5.4 nS), with a greater disparity when we stimulated the LR model cell (8.3 ± 0.6 nS) than when we stimulated the real cell (7.0 ± 0.2 nS). 2) Electrical loading of the action potential waveform was greater for real cell than for LR model cell even when real cell size was normalized to be equal to that of LR model cell. 3) When the size of the follower cell was doubled, required conductance for propagation was dramatically increased; but this increase was greatest for conduction from real cell to LR model cell, less for conduction from LR model cell to real cell, and least for conduction from LR model cell to LR model cell. The introduction of this "model clamp" technique allows testing of proposed membrane models of cardiac cells in terms of their source-sink behavior under conditions of extreme coupling by examining the symmetry of conduction of a cell pair composed of a model cell and a real cardiac cell. We have focused our experimental work with this technique on situations of extreme uncoupling that can lead to conduction block. In addition, the analysis of the geometrical factors that determine success or failure of conduction is important in the understanding of the process of discontinuous conduction, which occurs in myocardial infarction.

INTRODUCTION

The cardiac syncytium is comprised of an inhomogeneous, multidimensional assembly of electrically interconnected cells. It is appreciated that the membrane properties of the cells and the electrical connections among cells are spatially inhomogeneous throughout the heart. These normally occurring spatial inhomogeneities, including regions of automaticity, determine the normal excitation sequence of the heart. However, under conditions of myocardial infarction, further degrees of spatial inhomogeneity are imposed, with surviving cells grouped into patterns described as "mottled" such that discrete groups of cells are separated from other groups of cells by connective tissue (Spear et al., 1983; Gardner et al., 1985; Ursell et al., 1985; Fenoglio et al., 1983; Kienzle et al., 1987). Recent studies have emphasized the importance of the anatomical features of the infarct zone in producing slow conduction, which might be of significance in allowing reentrant activity to occur (de Bakker et al., 1993). Conduction delay has been observed as an apparently normal occurrence at junctions between Purkinje cells and the underlying subendocardial ventricular cells (Mendez et al., 1969; Veenstra et al., 1984), and at branching sites of bundles within the canine atrium (Spach et al., 1982). Conduction delay has also been created under various conditions of experimental imposition of either a resistive barrier of high effective intercellular resistance (Antzelevitch and Moe, 1983) or a narrow isthmus of surviving tissue connecting larger regions of tissue (De La Fuente et al., 1971). In studies utilizing isolated cells or cell pairs, conduction delay has been observed between two cells of a coupled cell pair of rat ventricular cells (Weingart and Maurer, 1988) or between two isolated guinea pig ventricular cells coupled by an electrical circuit with a variable coupling conductance (Sugiura and Joyner, 1992).

Studies to understand the mechanisms of the conduction delay and the determinants of success or failure of conduction, or of initiation of propagation in intact tissue, are complicated by the multiplicity of electrical interactions that may be occurring in a three dimensional syncytium and by the inability to determine the excitability properties of the individual cells. Numerous mathematical representations of the electrical activity of isolated ventricular cells have been produced that to some degree mimic the real electrical activity (Beeler and Reuter, 1977; Luo and Rudy, 1991, 1994a, b). We have used the most recent and comprehensive of these models (Luo and Rudy, 1994a) as a standard cell model and have coupled this model with a real-time simulation to real guinea pig ventricular cells using an extension

Received for publication 31 May 1995 and in final form 18 September 1995.

Address reprint requests to Dr. Ronald W. Joyner, Department of Pediatrics, Emory University, 2040 Ridgewood Drive NE, Atlanta, GA 30322. Tel.: 404-727-5747; Fax: 404-727-6024; E-mail: rjoyner@physiol.emory.edu.

0006-3495/96/01/281/15 $2.00

of a coupling circuit that we previously described (Tan and Joyner, 1990; Tan et al., 1991; Joyner et al., 1991; Sugiura and Joyner, 1992) as a "coupling clamp" technique. The introduction of this technique allows testing of proposed membrane models of cardiac cells in terms of their source-sink behavior under conditions of extreme uncoupling by examining the symmetry of conduction of a cell pair composed of a model cell and a real cardiac cell. However, we emphasize that this testing is limited to determining the ability of the model to account for conduction at values of junctional resistance near those that produce conduction failure. With this protocol, we have also investigated the effects of the relative size of the two cells of a cell pair on the success or failure of conduction, the required value of intercellular conductance, and the maximum conduction delay that could be created.

MATERIALS AND METHODS

Cell isolation

Single ventricular myocytes were isolated according to the method described in detail in our recent publications (Sugiura and Joyner, 1992; Kumar and Joyner, 1994). Adult guinea pigs of either sex weighing 300–500 g were anesthetized by 50 mg/kg pentobarbital sodium (Nembutal) and 500 units heparin i.p. The heart was rapidly removed via thoracotomy with artificial ventilation, and the aorta was cannulated for Langendorff perfusion. The isolated heart was mounted on a Langendorff apparatus and perfused sequentially with normal Tyrode's solution for 5 min, with nominally Ca^{2+} free Tyrode's solution for 6–7 min, with enzyme solution for 8–12 min, and with storage solution for 5 min, at a rate of 3–4 ml/g/min at 35–36°C. The ventricle was cut into small pieces, stirred in storage solution, filtered through nylon mesh, and stored in storage solution at room temperature. The isolated cells were transferred to an experimental chamber containing normal Tyrode's solution. The chamber was continuously perfused with normal Tyrode's solution at 2 ml/min and the temperature was maintained at 35 ± 0.5°C. Only cells that were quiescent and had a rod-shaped appearance were used in this study.

Solutions

Normal Tyrode's solution contained (in mM): NaCl, 148.8; KCl, 4.0; $CaCl_2$, 1.8; $MgCl_2$, 0.53; NaH_2PO_4, 0.33; HEPES, 5; glucose, 5; with pH adjusted to 7.4 using NaOH. The composition of nominally Ca^{2+}-free Tyrode's solution was the same as of normal Tyrode's solution except the $CaCl_2$ was omitted. The enzyme solution contained 4–6 mg/100 ml collagenase (Yakult, Tokyo, Japan) and 0.5 mg/100 ml protease (Type XIV, Sigma Chemical Co., St. Louis, MO) in nominally Ca^{2+} free Tyrode's solution. Storage solution had (in mM) K-glutamate 120, $MgCl_2$ 5, taurine 20, EGTA 0.5, glucose 10, HEPES 10, with pH adjusted to 7.4 using KOH. The composition of the internal pipette solution was (in mM): KCl, 135; Mg-ATP, 5; Na_2 creatine phosphate, 5.0; HEPES, 5.0; with pH adjusted to 7.2 using KOH. The external solution was normal Tyrode's solution.

Electrophysiological recording

Membrane potentials and currents were recorded using the whole-cell patch clamp technique (Hamill et al., 1981). The pipettes were pulled from borosilicate glass and, after fire-polishing, had resistances of 4–6 MΩ when filled with the internal solution. Relatively high-resistance patch pipettes were used to minimize intracellular dialysis. High-resistance seals were formed with the cell membrane using light suction, and the membrane was disrupted by applying a transient suction. Apart from zeroing the potential before touching the cell surface with the pipette tip, no attempts were made to correct for junction potential.

Recordings were made with an Axoclamp 2A dual amplifier (Axon Instruments, Inc., Foster City, CA) in the current clamp mode. To feedback the desired current to the headstage in our coupling clamp experiments (Fig. 1 *A*) we used the internal voltage-to-current (V-to-I) converter of the Axoclamp amplifier, with a command voltage of 1 V corresponding to a current input of 1 nA. Series resistance was carefully compensated for by internal bridge balance adjustments after recording of the membrane potential was established.

Current pulses of duration 2 ms and amplitude 10–15% suprathreshold were added to the stimulated cell at a frequency of 1 Hz. To determine the stimulus current threshold, we started with suprathreshold stimulus current magnitudes and gradually reduced the current magnitude until failure of activation occurred. We defined the input resistance for our cells as the amplitude of the voltage response produced by a small depolarizing current pulse of 20 ms duration, divided by the current amplitude. The current pulse was adjusted to produce membrane depolarizations 5–7 mV from the resting membrane potential and usually amounted to ~0.3 nA.

Cell model

The (phase 2) LR model for an isolated guinea pig ventricular cell has been published in detail (Luo and Rudy, 1994a). This model includes a mathematical representation of sarcolemmal ionic channel currents and pump currents, as well as a representation of calcium ion concentration with cytoplasmic buffers and the release and uptake of calcium by the sarcoplasmic reticulum (SR). The standard LR cell model has a membrane capacitance of 153.4 pF and an effective input resistance of ~21 MΩ, thus having an input time constant of ~3.3 ms. For numerical integration of differential equations we have applied the accurate and efficient method of Victorri et al. (1985) with a fixed time step, Δt. All software was compiled as a DOS real mode application using Turbo Pascal (version 7.0, Borland International, Inc., Scotts Valley, CA) on IBM AT-compatible computers. Several actions were taken to speed up calculations in the real-time solution of the LR model: 1) All computations were performed using the 4-byte "single" variable format of the computer's floating point unit, i.e., with a degree of precision of 7–8 decimal figures, instead of the 10-byte "extended" format. 2) We fixed the intracellular sodium and potassium ion concentrations, which do not change noticeably during the course of an action potential, to their initial values of 10 and 145 mM (Luo and Rudy, 1994a), respectively. 3) Steady-state values of gating variables d, f, h, j, m and x, as well as the expressions $\exp(-\Delta t/\tau)$ involving their time constants τ, were taken from lookup tables. Values were stored for membrane potentials, V_m, from −100 to +60 mV in 0.25-mV increments. 4) Similarly, lookup tables, also in 0.25-mV increments, were used for V_m-dependent expressions appearing in the equations for the calcium, potassium, and sodium components of the L-type calcium current (I_{Ca}, I_{CaK}, and I_{CaNa}, respectively), the time-dependent potassium current (I_K), the sodium-calcium exchanger (I_{NaCa}), the nonspecific calcium-activated current ($I_{NS(Ca)}$), and the total time-independent current (I_V). 5) From the equations for calcium buffer concentrations, which were computed under the steady-state assumption (Luo and Rudy, 1994a), it follows that the free calcium concentration in the myoplasm, $[Ca^{2+}]_i$ can be calculated from the total calcium concentration in the myoplasm, $[Ca^{2+}]_{i,tot}$, according to

$$[Ca^{2+}]_i = -5.8407 * 10^{-5} + [Ca^{2+}]_{i,tot} * (0.012799 + [Ca^{2+}]_{i,tot} * ([Ca^{2+}]_{i,tot} * 3.8692 - 0.17534)),$$

where both $[Ca^{2+}]_i$ and $[Ca^{2}]_{i,tot}$ are in mM. We first computed $[Ca^{2+}]_{i,tot}$ from the equations for calcium currents and fluxes, and then computed $[Ca^{2+}]_i$ from the above equation. 6) Similarly, the free calcium concentration in the junctional SR (JSR), $[Ca^{2+}]_{JSR}$ was calculated from the total calcium concentration in the JSR, $[Ca^{2+}]_{JSR,tot}$, according to

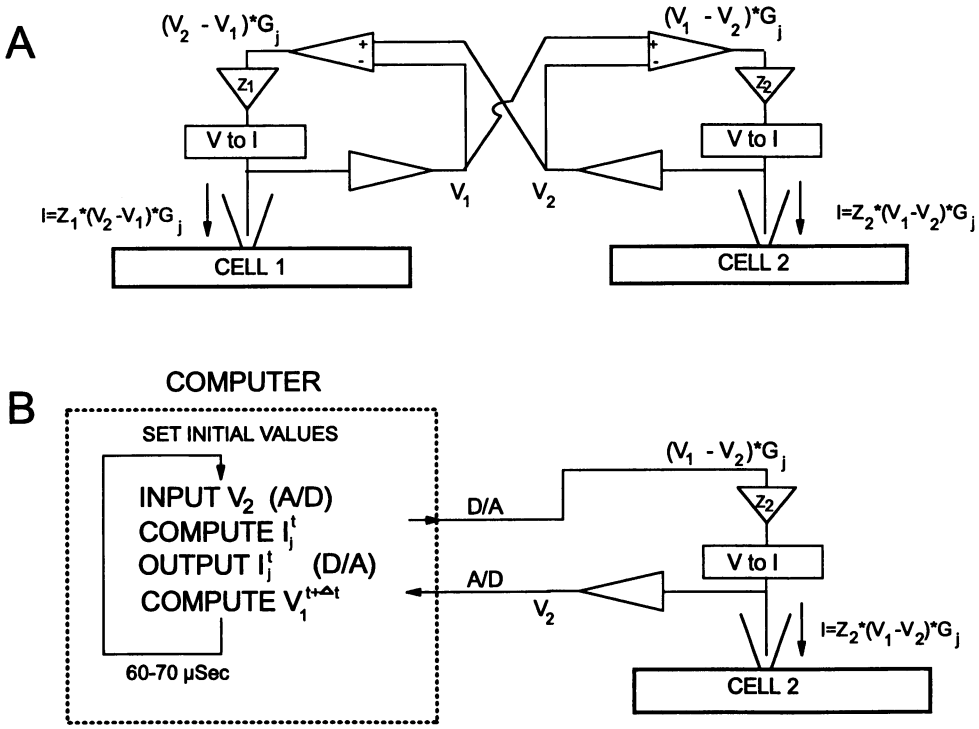

FIGURE 1 Experimental techniques to study how two physically unconnected cells interact with each other when they are electrically coupled with a variable coupling conductance, G_j, and with experimentally variable effective cell size (proportional to $1/Z_1$ for cell 1 and to $1/Z_2$ for cell 2). *A*) Analog "coupling clamp" technique. Membrane potentials V_1 and V_2 of two isolated cells, cell 1 and cell 2, respectively, are recorded using a dual amplifier in the current clamp mode. Two additional amplifiers continuously compute $V_2 - V_1$ and $V_1 - V_2$, respectively, using an effective gain such that the V-to-I converters continuously supply currents $G_j * (V_2 - V_1) * Z_1$ and $G_j * (V_1 - V_2) * Z_2$ to cell 1 and cell 2, respectively, i.e., the currents that would have been conducted through a real intercellular conductance G_j. *B*) "Model clamp" technique. Cell 1 of *A* has been replaced with a mathematical model cell. The membrane potential of the real cell, V_2, is recorded using an amplifier in the current clamp mode, and sampled into a microcomputer. The coupling current, $I_j = G_j * (V_1 - V_2)$, is computed and a command voltage is generated such that a current input $I_j * Z_2$ is supplied to the real cell, cell 2. The membrane potential of the model cell, V_1, is computed from the mathematical model with the current input for this cell, $-I_j * Z_1$, as an additional ionic current.

$$[Ca^{2+}]_{JSR} = -0.047671 + [Ca^{2+}]_{JSR,tot} * (0.11596 + [Ca^{2+}]_{JSR,tot} * ([Ca^{2+}]_{JSR,tot} * 0.0019814 - 0.0062985)),$$

where both $[Ca^{2+}]_{JSR}$ and $[Ca^{2+}]_{JSR,tot}$ were in mM. We verified that the above time-saving optimizations did not affect our results by running the model with and without these optimizations for time steps between 1 and 70 μs (data not shown).

Model clamp

Using a 90-MHz Pentium processor computer equipped with a fast 12-bit data acquisition board (Digidata 1200, Axon Instruments) we have incorporated the "model clamp" technique (Fig. 1) with the LR ventricular cell model with a time step of 70 μs, i.e., with a sample frequency of ~14 kHz. In our standard protocol for the LR model, the program runs without coupling to the real cell for 2 s, then establishes coupling at a desired value of intercellular conductance for a variable number of seconds, then finishes the run with again a 2-s period of uncoupling. The program also incorporates periodic activation, if desired, of the LR model cell at a variable rate. The computer program stores as an array the successive samples of the membrane potential of the real cell. At the end of the run, data are displayed and the samples are transferred to disk, together with parameter settings. With this information, a second program can then off-line "replay" the experimental protocol, producing a disk file with a time sequence of the membrane potential of the real cell, the membrane potential of the model cell, the coupling current, and any computed parameters of the model cell, e.g., cytoplasmic calcium concentration, as functions of time. Although our method allows the specification of junctional conductance as a function of intercellular voltage difference or of concentrations of specific ions, for the present studies we have not included any voltage, pH, or calcium dependence of junctional conductance.

Coupling a guinea pig ventricular cell to a simulated ventricular cell

The coupling circuit we are using has been previously described for coupling a ventricular cell to an RC circuit (Tan and Joyner, 1990; Tan et al., 1991; Kumar and Joyner, 1994) or to another ventricular cell (Joyner et al., 1991; Sugiura and Joyner, 1992). We now extend this method to couple a guinea pig ventricular cell to a simulated cell model. We are recording from an isolated guinea pig ventricular cell in the "current clamp" mode with the ability to pass current into the cell based on a computed coupling current that would have been present if the cell were actually coupled by a given conductance to the LR model cell. Simultaneously, the computed coupling current is being applied to the LR model computations. All of our records then are recordings from the real cell with simultaneously generated model solutions. Because the LR model has a standard size and real ventricular cells do not, it is important to define some method of standardizing the "size" of the real cell and of the LR model cell. The strength-duration relationship for ventricular cells compares well with the strength-duration curve for the LR model when the current threshold for a 2-ms duration stimulus is normalized to the 2.6 nA value for the LR

model (see below). We define the standard size of a cell in terms of the current threshold (2 ms duration). Thus, if the current threshold is 5.2 nA, then the size of the cell is considered to be twice that of the LR model cell. Conversely, if we scale the size of the LR model cell up by a factor of 2, then the size of the cell and the size of the LR model would again be the same. The procedure we have used is as follows: we first record the current threshold for the cell, I_{th}, and we then use a size factor of $I_{Ah}/2.6$ for the LR model simulation as a standard factor throughout the experiment such that the relative sizes of the cell and the LR model are the same, with the current threshold of both real cell and model cell amounting to I_{th}. During the experiment on a given cell, we then further scale either the real cell size or the LR model cell size to systematically alter the relative size of either the real cell or the LR model. For our experimental system, we can apply repetitive stimulus pulses to the real cell and/or the LR model cell. We define the cell of the cell pair that is receiving the stimulus as the "leader" and the other cell as the "follower". To account for the varied cell sizes during the experiments, with the current threshold of the standard cell (size 1) amounting to I_{th}, we have normalized all of the intercellular conductance values by dividing by the above factor of I_{th} 2.6. It is important to note that we are changing the effective size of the LR model, or of the real cell, by scaling the coupling. Thus, with respect to all calculations for the LR model that involve the cell volume or surface area, or that of intracellular compartments, no alterations need to be made to accomplish the change in the effective cell size.

Fig. 1 illustrates the experimental procedure. Fig. 1 *A* illustrates the analog coupling clamp we have previously used (Sugiura and Joyner, 1992). An amplifier system does a continuous analog computation of the current that would be flowing into or out of each cell if there had been a intercellular coupling conductance G_j between the two cells. If V_1 is the time-varying membrane potential of cell 1 and V_2 is the time-varying membrane potential of cell 2, then there would be a time-varying coupling current I_j flowing from cell 1 to cell 2 (positive or negative) given by $I_j = G_j * (V_1 - V_2)$. Two amplifiers continuously compute $V_2 - V_1$ and $V_1 - V_2$, respectively. The outputs of these amplifiers go through V-to-I converters and then back to the cells to provide the current inputs to cell 1 and cell 2 that would have been conducted through a real intercellular conductance G_j (Fig. 1 *A*). The specification of the value of G_j is a combination of the fixed gain of the V-to-I converters and the variable gain of the two amplifiers. An analog cell model, e.g., an RC circuit, may be substituted for one of the cells and connected to the headstage of the dual amplifier (Tan and Joyner, 1990; Tan et al., 1991). Replacing real cell 1 in the analog coupling clamp system of Fig. 1 *A* with a mathematical model of this cell, we obtain the model clamp system of Fig. 1 *B*. In this system, the membrane potential of cell 1 is not recorded from a real cell, but computed from a detailed mathematical model of an isolated cell. We define two additional parameters Z_1 and Z_2 as scaling factors for the currents applied to either the model cell or the real cell to effectively alter the size of the model cell and the real cell. A current input $I_j * Z_2$ is supplied dynamically to the real cell (cell 2) to produce the effect of the (mutual) interaction with the model cell (cell 1) whereas the membrane potential of the model cell, V_1, is computed with the current input for this cell, $I_j * Z_1$, as an additional ionic current to produce the effect of the (mutual) interaction with the real cell.

Statistical analysis

For each real ventricular cell studied, we analyzed the critical junctional conductance and the maximal conduction delay for the conditions of stimulation of either the real cell or the cell model with the sizes of the real cell and the cell model adjusted as shown in Tables 1 and 2. Statistical analysis was performed with ANOVA followed by pairwise comparisons with the Tukey HSD test with a significance level of $p < 0.05$.

RESULTS

Effects of the time step on LR model solutions

Because the LR model contains some components that have fast kinetics, viz. the sodium and calcium channel currents, it is to be expected that the time step of 70 μs imposed by our model clamp hardware would alter the time course of some of the computed conductances and thus the time course of membrane potential. Fig. 2 contrasts the results obtained when the LR model is solved for a time step of 1 μs (*dashed lines*) versus a time step of 70 μs (*solid lines*). Fig. 2 *A* shows the complete action potential with excellent correspondence for the two solutions. As shown at a faster time scale in Fig. 2 *B* for the initial phase of the action potential, the solution with the 70-μs time step has an action potential peak amplitude of 3.8 mV too high, but is otherwise nearly identical with the solution at the 1-μs time step. The lower panels of Fig. 2 show the computed waveforms for the sodium and for the calcium channel currents. Note that we have used $I_{Ca,t}$ to indicate the current through the calcium channel. In the LR model (Luo and Rudy, 1994 a, b) formulation, the current through this channel is primarily carried by calcium ions, but also has some contribution of sodium and potassium ions. Our results for $I_{Ca,t}$ can be compared to their figure 17 *A*. The sodium channel current has a peak value of ~420 pA/pF for the 70-μs time step, whereas the peak value for the 1-μs time step amounts to ~380 pA/pF. For the calcium channel current, the waveform is nearly the same over all of the action potential time course except for the first few milliseconds, when the solution for the shorter time step has a higher amplitude (Fig. 2 *D*): 3.7 pA/pF versus 2.9 pA/pF for the 70-μs time step.

Because we are particularly interested in the application of this model for conduction studies, we needed to also check the effect of the time step used on the potential and current waveforms when the model is subjected to the

TABLE 1 Effects of follower and leader size on critical conductance (nS) with either model to real cell, real cell to model, or model to model conduction

	LR model cell to real cell	Ratio to equal size	Real cell to LR model cell	Ratio to equal size	LR model cell to LR model cell	Ratio to equal size
Equal size	8.3 ± 0.6 (8)*		7.0 ± 0.2 (8)		5.4	
Follower × 2	21.8 ± 2.3 (7)‡	2.6 ± 0.2*	24.2 ± 1.7 (7)‡	3.5 ± 0.2	12.7	2.35
Follower × 0.5	4.0 ± 0.3 (8)‡,*	0.5 ± 0.02*	2.9 ± 0.1 (8)‡	0.4 ± 0.01	2.5	0.46
Leader × 2	7.8 ± 0.6 (6)*	0.9 ± 0.01*	5.6 ± 0.2 (5)‡	0.8 ± 0.01	5.0	0.93
Leader × 0.5	11.5 ± 1.2 (6)‡	1.3 ± 0.05*	12.5 ± 1.4 (4)‡	1.8 ± 0.1	6.4	1.19

*Significant difference for "model stimulation" versus "cell stimulation."
‡Significant difference compared to "equal size" for the same stimulus. Numbers in parentheses indicate number of experimental observations.

TABLE 2 Effects of follower and leader size on maximal conduction delay (ms) with either model to real cell, real cell to model, or model to model conduction

	LR model cell to real cell	Ratio to equal size	Real cell to LR model cell	Ratio to equal size	LR model cell to LR model cell	Ratio to equal size
Equal size	31.2 ± 0.8 (8)*		24.3 ± 1.4 (8)		45	
Follower × 2	20.4 ± 1.4 (7)‡,*	0.7 ± 0.04*	12.9 ± 0.8 (7)‡	0.5 ± 0.03	39	0.87
Follower × 0.5	33.7 ± 1.8 (8)	1.1 ± 0.06	30.7 ± 3.1 (8)‡	1.3 ± 0.12	49	1.09
Leader × 2	34.9 ± 2.5 (6)	1.1 ± 0.08	34.0 ± 2.9 (5)‡	1.4 ± 0.2	49	1.09
Leader × 0.5	21.3 ± 2.2 (6)‡,*	0.7 ± 0.06*	12.2 ± 1.0 (4)‡	0.5 ± 0.03	39	0.87

*Significant difference for "model stimulation" versus "cell stimulation."
‡Significant difference compared to "equal size" for the same stimulus. Numbers in parentheses indicate number of experimental observations.

electrotonic load of an adjacent cell. As an analytical approach to this situation, we first coupled the LR model to a second model cell that had the same resting potential but was represented as a parallel combination of a 20-MΩ resistor and a capacitor of 153 pF, which corresponds to the input resistance and input capacitance for the LR model. As shown in Fig. 3 *A*, the effects of coupling this model cell to the LR model by a junctional conductance of 10 nS produced a dramatic shortening in the action potential duration and a small decrease in the peak amplitude. However, as shown at a faster time scale in Fig. 3 *B*, the difference between the solution at a time step of 1 μs and that at a time of 70 μs still only 4.2 mV. The sodium and calcium channel currents are shown in Fig. 3, *C* and *D*, for this loading condition. The sodium channel current is minimally affected by the electrical load, but the calcium current is dramatically increased in magnitude and shortened in duration. However, the effects of this loading on the sodium and calcium current are very similar for the time steps used.

Determination of cell size

A straightforward method to obtain the size of a ventricular cell would be to determine its stimulus current threshold. Therefore, it is important first to document the excitability of both the real cell and the LR model with respect to the duration of the stimulus. Fig. 4 shows results from six isolated guinea pig ventricular cells for which we recorded the threshold current for stimulation at a periodic 1-Hz rate as functions of the duration of the stimulus. Because of the experimental variation in the size of the cells, there is a wide variation in the amplitudes of the required currents, as shown in Fig. 4 *A*. However, when we normalized each of the experimental curves such that the value at 2 ms is equal to the current threshold for a 2-ms duration of the LR model (2.6 nA) and then compared the means of the experimental data for each duration with the computed results for the LR model for each duration, we got the results shown in Fig. 4 *B*. The strength-duration curves are quite similar for the

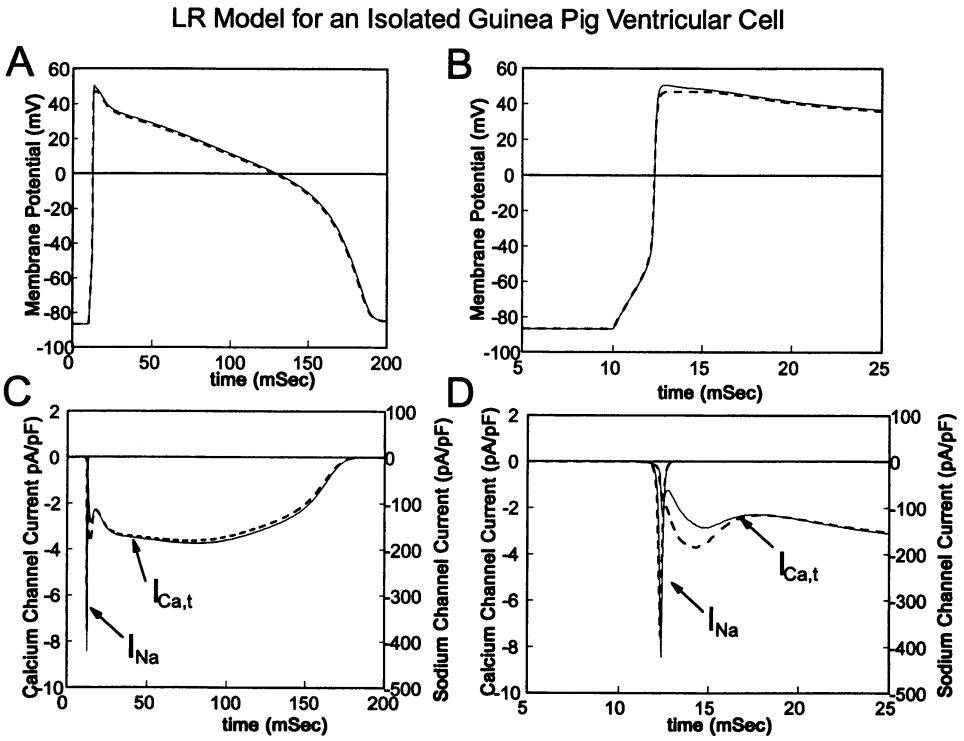

FIGURE 2 LR model (Luo and Rudy, 1994a,b) of a guinea pig ventricular cell solved for time steps of 70 μs (*solid lines*), using single-precision arithmetic and lookup tables, and 1 μs (*dashed lines*). The LR model cell was stimulated with current pulses of duration 2 ms and amplitude 3.0 nA at a frequency of 1 Hz. *A*, *B*—Membrane potential. *C*, *D*—Calcium channel current ($I_{Ca,t}$) and sodium channel current (I_{Na}). Note different ordinate scales.

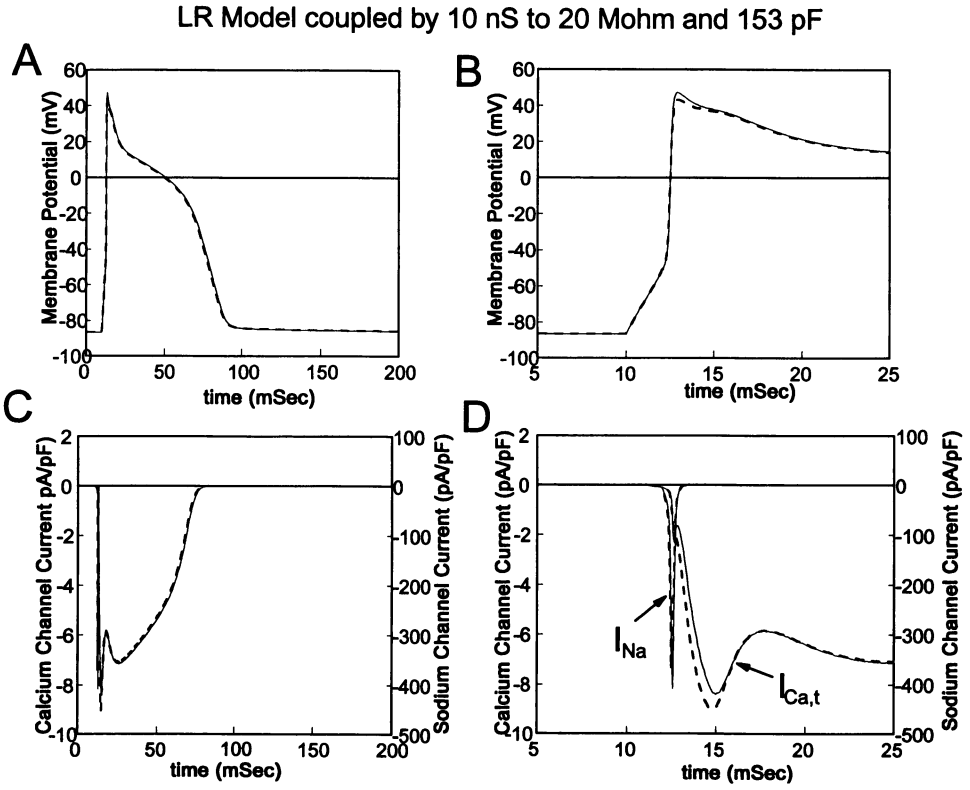

FIGURE 3 LR model (Luo and Rudy, 1994a,b) of a guinea pig ventricular cell coupled to a passive RC model solved for time steps of 70 μs (*solid lines*) using single-precision arithmetic and lookup tables, and 1 μs (*dashed lines*). Coupling conductance was 10 nS. Resistance and capacitance of the RC model were 20 MΩ and 153 pF, respectively. The RC model was given an offset potential equal to the resting potential of the model cell. The LR model cell was stimulated with current pulses of 2 ms in duration and amplitude 3.0 nA at a frequency of 1 Hz. *A, B*—Membrane potential. *C, D*—Calcium channel current ($I_{Ca,t}$) and sodium channel current (I_{Na}). Note different ordinate scales.

experimental data and the LR model data, with the predominant difference being that, for longer durations, the LR model has a greater decrease in current threshold than the real guinea pig cells.

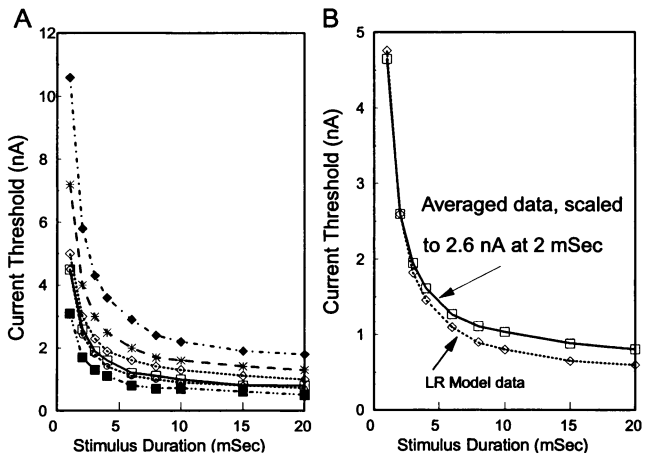

FIGURE 4 *A* and *B* are stimulus current strength-duration relation of the LR guinea pig ventricular cell model versus six real isolated guinea pig ventricular cells. *A* shows stimulus-current threshold as a function of stimulus duration for stimulation of an isolated guinea pig ventricular cell at a frequency of 1 Hz. Different symbols indicate different cells. *B* shows the mean strength-duration relation of the isolated cells after normalizing the data from each cell such that the current threshold at 2 ms in duration is 2.6 nA (*squares*), and the strength-duration relationship of the LR model cell (*diamonds*).

Validity of the model system

Because we are particularly interested in studying the conduction of action potentials between the model cell and the real cell, it was important to assess the validity of the model system in representing the loading effects of coupling to a passive load. This was assessed in three ways. First, as in Fig. 3, we expanded the model system to incorporate a theoretical representation of two cells, in which one model cell was the LR model and the other model cell was represented by a mathematical representation of a 20 MΩ resistor in parallel with a 150 pF capacitor with an offset voltage equal to the resting potential of the LR model. In this case we computed, at each 70-μs time step, the "membrane current" of each model cell and used this plus the coupling current to integrate the potential of each model cell, and then used these potentials to compute the coupling current (based on a coupling conductance of 10 nS) to be subtracted from the LR model cell and added to the theoretical RC Model cell for the next time step. For the second assessment, we used the model clamp circuit as shown in Fig. 1 *B* to couple the theoretical LR model cell to a physical model of an RC circuit (a real 20 MΩ resistor and a real 150 pF capacitor) connected to the headstage of the Axoclamp amplifier and given an offset voltage equal to the resting potential of the LR model. For this case, we computed the effects on the LR model cell of the interactions with the physical RC circuit, also using a time step of 70 μs and a coupling conductance of 10 nS. For the third assessment, we

used the analog coupling clamp circuit of Fig. 1 *A* with a real guinea pig ventricular cell recorded with a pipette via one headstage of the Axoclamp amplifier and the physical RC circuit inserted into the other headstage of the Axoclamp amplifier to see how the same physical RC circuit would load the real cell compared to its loading effect on the model cell.

The first and second assessments are essentially tests of the validity of our system as a means to accurately implement the coupling currents that would be flowing between two coupled cells. Fig. 5 *A* shows the results when the LR model was coupled by 10 nS to a computed RC model with 20 MΩ and 150 pF (*solid lines*), and when the LR model was coupled through the circuit shown in Fig. 1 *B* to a real RC circuit with a 20 MΩ resistor and a 150 pF capacitor connected to the headstage of the Axoclamp amplifier (*dotted lines*). Results are plotted for the uncoupled solution, the solution for the LR model when loaded, and the solution (*solid line*) or actual recording (*dotted line*) for the RC model.

Fig. 5 *B* shows an example of the use of our analog coupling clamp circuit (Fig. 1 *A*) to couple a real guinea pig ventricular cell to the same RC circuit used for the computations of Fig. 5 *A*. The cell used for this experiment was chosen as the one with the current threshold (2.4 nA) from the ones recorded that was most similar to the LR model current threshold of 2.6 nA. The results are generally similar for the real cell as compared to the LR model, although we consistently found that the real cells have greater action-potential-duration shortening with an electrical load than that expressed by the LR model.

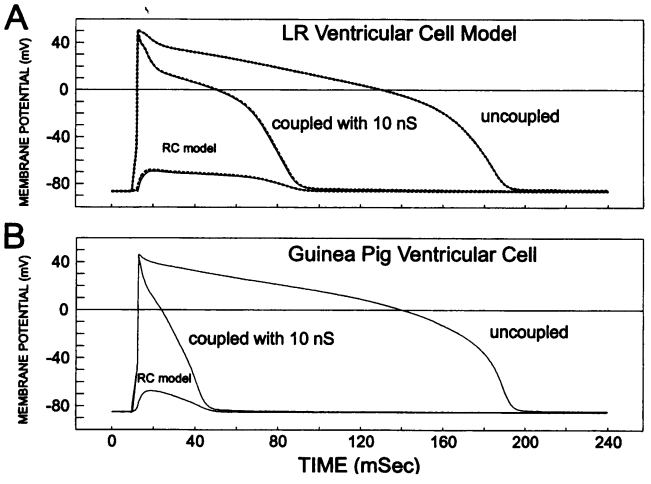

FIGURE 5 *A* and *B* test the validity of the ventricular cell model system in representing the loading effects of coupling to a passive load. *A* shows the solution of the LR model of a guinea pig ventricular cell solved for a time step of 70 μs, when uncoupled and when coupled either to a computed RC model (*solid lines*) or to a real RC circuit connected to the headstage of the amplifier (*dotted lines*). Coupling conductance was 10 nS. Resistance and capacitance of both the RC model and the RC circuit were 20 MΩ and 150 pF, respectively. Both the RC model and the RC circuit were given an offset potential equal to the resting potential of the LR model cell. The LR model cell was stimulated with current pulses of 2 ms in duration and amplitude 3.0 nA at a frequency of 1 Hz. *B* shows an action potential of an isolated guinea pig ventricular cell when uncoupled and when coupled to the same RC circuit using the coupling clamp circuit of Figure 1 *A*. Coupling conductance was 10 nS. Resistance and capacitance of the RC circuit were 20 MΩ and 150 pF, respectively. The RC circuit was given an offset potential equal to the resting potential of the isolated cell. The isolated cell had a current threshold of 2.4 nA at a stimulus duration of 2 ms, and was stimulated with current pulses of duration 2 ms and amplitude 2.6 nA at a frequency of 1 Hz.

Effects of cell size on conduction properties

The large variation in ventricular cell size that is experimentally found represents an experimental problem and an opportunity to study the effects of cell size on conduction properties. The inclusion in our model clamp system of the ability to change the effective size of the model cell or the real cell (Fig. 1) is necessary for normalization of the results. For 19 ventricular cells that we used for this study, the current threshold for a 2-ms duration stimulus ranged from 1.5 to 4.1 nA, with a mean ± SEM of 2.48 ± 0.17 nA. The average values of input resistance and input capacitance of these cells were 25.9 ± 3 MΩ and 85 ± 8 pF, respectively. These are not presented as "average" values for guinea pig ventricular cells, because we purposely selected smaller than average cells from the dissociation to minimize problems with residual series resistance. Fig. 6 illustrates the use of this ability to change the effective size of either the leader or the follower cell of a ventricular cell pair. For an analytical demonstration, we used the LR model coupled

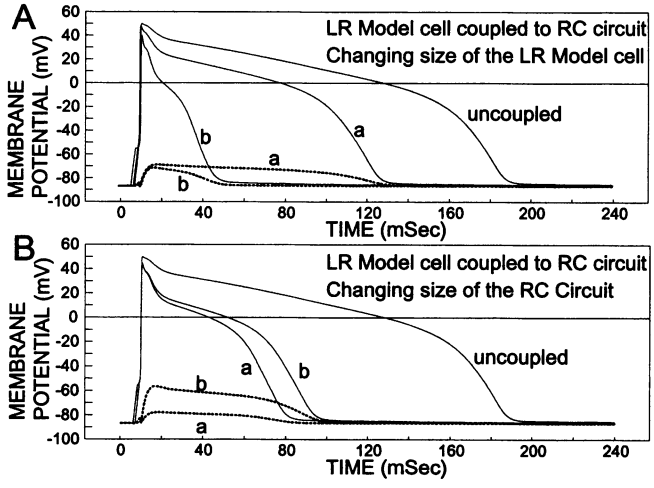

FIGURE 6 Analytical demonstration of the effects of cell size on conduction properties. Action potential of the LR model of a guinea pig ventricular cell solved for a time step of 70 μs, when uncoupled and when coupled to a RC circuit using the model clamp circuit of Figure 1 *B*. Coupling conductance was 10 nS. Resistance and capacitance of the RC circuit were 20 MΩ and 150 pF, respectively. The RC circuit (*dotted lines*) was given an offset potential equal to the resting potential of the LR model cell. The LR model cell (*solid lines*) was stimulated with current pulses of duration 2 ms and amplitude 3.0 nA at a frequency of 1 Hz. *A*—Size of LR model cell increased (*curves* labeled 'a') or decreased (*curves* labeled 'b') by a factor of two. *B*—Size of RC circuit increased (*curves* labeled 'a') or decreased (*curves* labeled 'b') by a factor of two.

by 10 nS to the same physical RC circuit as before. For Fig. 6, *A* and *B* the solid lines are the LR model results and the dotted lines are recordings from the RC circuit. The action potential waveform without coupling is shown in each panel for reference. For the waveforms labeled "a" in Fig. 6 *A* we increased the size of the LR model cell by a factor of 2, and for the curves labeled "b" we reduced the size of the LR model cell by a factor of 2. The passive load encountered by the LR model cell is the series combination of the 10 nS coupling conductance and the input conductance of the RC circuit. The results for the waveforms of the LR model cell can be compared to the results of Fig. 5 when the size of the LR model cell was not changed. Note that the changes in the size of the LR model cell, which in this case is the leader cell, i.e., the cell being stimulated, have minimal effects on the amplitude of the potential recorded from the RC circuit model. However, increasing the size of the LR model cell (leaving the size of the passive load unchanged) makes the passive load have less effect on the action potential duration of the LR model cell. Conversely, when the size of the LR model cell is decreased, the action potential shortening is increased (curves labeled "b"), because the effective input resistance of the LR model cell has now been increased with respect to the passive load.

The results are not the same when we make the changes in size for the RC circuit rather than for the LR model. Fig. 6 *B* shows results for a doubling in the size of the RC circuit (labeled "a") and halving in the size of the RC circuit (labeled "b"). It is important to note here that doubling the size of the RC circuit, which is accomplished in the model clamp circuit of Fig. 1 *B* by setting Z_2 to 0.5, makes the effective values of R and C equal to 10 MΩ and 300 pF, respectively, maintaining the same time constant, τ (R * C). Thus, the effects of changing the size of the RC circuit are seen mostly in the amplitude of the recordings from the RC circuit and the differences in action potential duration of the LR model cell produced by changing the size of the RC circuit are small.

Fig. 7, *A* and *B* illustrates the correspondence between a recorded guinea pig ventricular cell action potential (*solid line*) and the simulated results of the LR model cell (*dotted line*) when each is uncoupled from the other. The action potential duration is quite similar, with the action potential plateau being somewhat higher for the real cell. The resting membrane potential and the action potential peak amplitude also correspond very well. Of course, the results for real cells vary somewhat in all these parameters, but this correspondence was typical of the results obtained. This particular cell had a current threshold of 1.7 nA and was used for all of the interventions described in Figs. 7–9. When two LR model cells are interconnected by a variable conductance G_j the conduction delay increases as G_j decreases and conduction failure occurs below a critical value of G_j, which for two LR model cells is 5.4 nS. We applied an experimental procedure of systematically varying G_j for coupling between the LR model cell and the real cell, and obtained the results shown in Fig. 7 when the stimulus was alternatively applied to either the LR model cell (Fig. 7 *C*) or to the real cell (Fig. 7 *D*) with the size of the LR model and the real cell adjusted to be the same. Each of these panels illustrate the maximal delay obtained at a value of G_j below which conduction failed. This value of critical G_j was 8.4 nS for conduction from the model cell to the real cell and was 6.7 nS for conduction from the real cell to the model cell. For

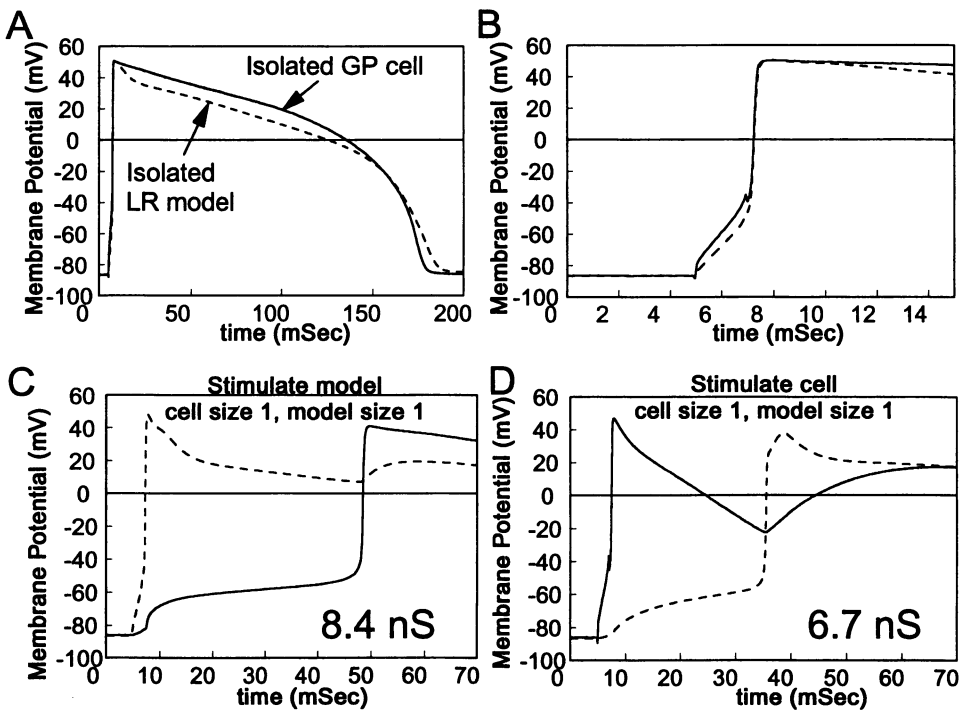

FIGURE 7 *A* and *B* are plots comparing an action potential recorded from a guinea pig ventricular cell ("Isolated GP cell," *solid line*) with the simulated result of the LR model simulation ("Isolated LR model," *dotted line*) shown at a slow (*A*) and a fast (*B*) time scale. GP cell 8–15-94–4. *C* and *D* are plots comparing the action potential recorded from the same isolated guinea pig ventricular cell (*solid line*) to the simultaneously produced LR model solution (*dotted line*) when the LR model was connected to the real cell by a conductance as indicated in the lower right corner of each panel, that, for each panel, was the lowest coupling conductance for which conduction was successful. For *C* the periodic stimulus (1-Hz frequency) was applied to the LR model stimulation, whereas for *D* the periodic stimulation was applied to the real cell. For both *C* and *D* the cell size has been adjusted to be equal to the standard size of the LR model simulation, based on the determination of the current threshold for the real cell for a stimulus duration of 2 ms.

8 cells in which we applied this protocol (Table 1), the averaged values (mean ± SEM) were 8.3 ± 0.6 nS for conduction from the model cell to the real cell and 7.0 ± 0.2 nS for conduction from the real cell to the model cell, with the required conductance for the direction from model cell to real cell being significantly higher. Several other differences are apparent from the figure. One major distinction is that the electrical loading occurring during the conduction process produces much more partial repolarization on the real cell when the real cell is the leader (Fig. 7 *D*) than on the model cell when the model cell is the leader (Fig. 7 *C*), even when the size of the two cells has been adjusted to the same value and the action potential peak amplitude and early plateau (when uncoupled, see Fig. 7 *A* and *B*) are either equal or higher for the real cell compared to the model cell. The significant partial repolarization of the real cell during the conduction process actually limits the conduction delay because the real cell is becoming a less effective source of current as the potential of the real cell progressively decays during the conduction process. Note also that the action potential peak amplitude of the LR model cell or the real cell, when serving as a follower, is lower than that obtained when the same cell is serving as a leader, and this effect is more pronounced for the model cell than for the real cell under these conditions of equal cell size.

To investigate the effects of changes in the cell size, there are two variables that must be systematically varied: 1) whether the model cell or the real cell is the leader receiving the direct stimulation; and 2) whether the change in cell size is being made for the leader cell or the follower cell. As in Fig. 7, the results shown in Fig. 8 and 9 (using the same real ventricular cell as for Fig. 7) illustrate the conduction process at the minimum value of G_j for which conduction was successful. Fig. 8, *A* and *B*, shows results obtained for stimulating the model cell when we had either doubled the size of the real cell (Fig. 8 *A*) or halved the size of the real cell (Fig. 8 *B*). Note that these size changes are in the follower cell of this pair. Compared with the conditions of stimulation of the model cell when the two cells are of the same size (Fig. 7, *C* and *D*) the results for Fig. 8 *A* show that when the size of the follower cell is increased a greater value of G_j is required for successful conduction (22.9 nS versus the 8.4 nS required for conduction from the model cell to the real cell with equal cell sizes). In addition, the electrical loading on the leader cell is increased by increasing the size of the follower cell, as indicated by the greater degree of partial repolarization during the conduction pro-

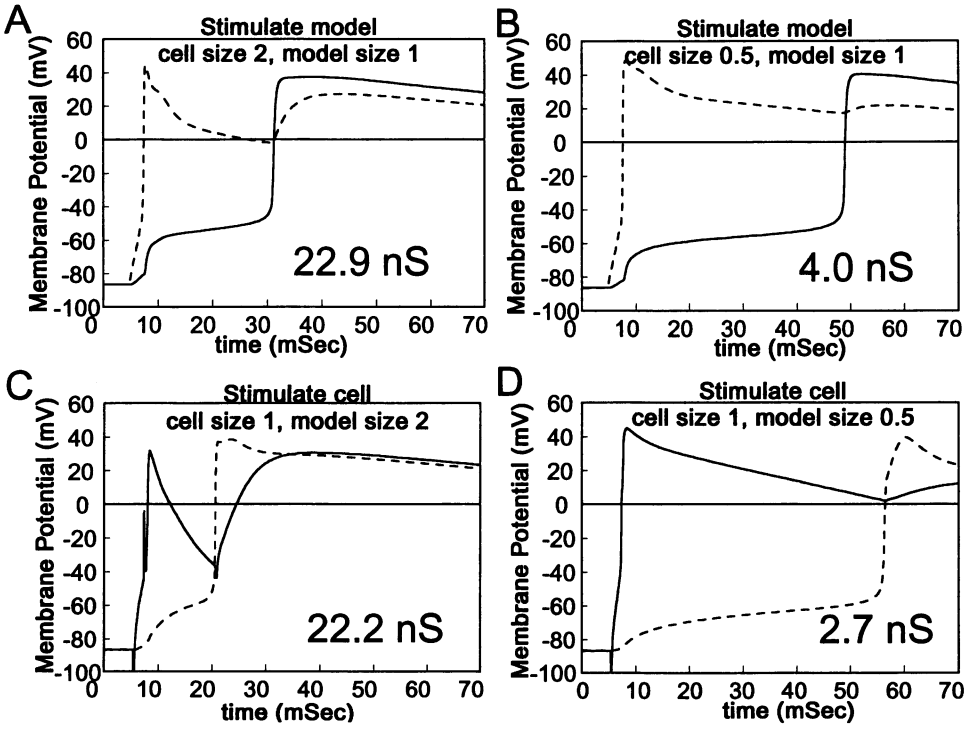

FIGURE 8 Effects of changing the size of the follower cell on conduction properties. *A* and *B* are plots comparing the action potential recorded from an isolated guinea pig ventricular cell (*solid line*) with the simultaneously produced LR model solution (*dotted line*) when the LR model was connected to the real cell by a conductance as indicated in the lower right corner of each panel that, for each panel, was the lowest coupling conductance for which conduction was successful. For *A* and *B* the periodic stimulus (1-Hz frequency) was applied to the LR model cell. For these two parts the real cell (follower cell) size has been adjusted to be either double that of the LR model cell (*A*) or half the size of the LR model cell (*B*), based on the determination of the current threshold for the real cell for a stimulus duration of 2 ms. *C* and *D* show the results when the periodic stimulus (1-Hz frequency) was applied to the real cell. For these two parts the LR model cell (follower cell) size has been adjusted to be either double that of the standard LR model cell size (*C*) or half the size of the standard LR model cell size (*D*); whereas the size of the real cell is adjusted to be equal to the standard LR model cell size, based on the determination of the current threshold for the real cell for a stimulus duration of 2 ms.

cess. Because the partial repolarization tends to limit the conduction process, the maximum conduction delay is decreased from 40 ms to 20 ms. The results shown in Fig. 8 *B* show that the effects of halving the size of follower cell are a decrease in the required conductance from 8.4 nS to 4.0 nS and a decrease in the loading effects on the leader cell. For seven cells in which we tested this particular paradigm, the average critical conductance was 21.8 ± 2.3 nS when the model cell was stimulated and the size of the real cell was doubled, and was 4.0 ± 0.3 nS when the size of the real cell was halved, with both values significantly different from the value obtained with equal sizes of the model and the cell.

When we then stimulated the real cell and repeated the process of doubling or halving the size of the follower cell (now the model cell), we got the results shown in Fig. 8, *C* and *D*. Fig. 8 *C* shows, with doubling of the size of the follower cell, a tremendous early repolarization of the real cell (the leader) and an increase in the required coupling conductance to 22.2 nS. The results are qualitatively the same as when the follower size was doubled with the model cell as the leader (Fig. 8 *A*) but, as we observed for conduction with the same cell size (Fig. 7, *C* and *D*), the electrical loading effects on the real cell are much more substantial than for the model cell. In seven cells for which we applied this experimental paradigm, the average required conductance was 24.2 ± 1.7 nS, significantly higher than the value obtained for conduction from the real cell to the model cell with equal size. When we now halved the size of the model cell, continuing to stimulate the real cell, we obtained the results shown in Fig. 8 *D*. Now, compared with the results obtained with equal cell size, the extent of the early repolarization of the leader cell is decreased and the maximum delay is increased, with a corresponding decrease in the critical conductance value to 2.7 nS. When we applied this protocol to 8 cells, we obtained an average value of 2.9 ± 0.1 nS for critical conductance when the real cell was stimulated and the size of the model cell was halved, significantly lower than the value obtained when the cell sizes were the same and when the model cell was stimulated and the real cell size was halved.

We then investigated the effects of changing the size of the leader of a cell pair when the leader was either the model cell or the real cell. Fig. 9 *A* shows results obtained when the model cell was stimulated with the size of the model cell doubled. Compared to the results obtained when the two cells were the same size (Fig. 7 *C*) there is now a decrease in the required coupling conductance to 7.7 nS and noticeably less early repolarization during the conduction process.

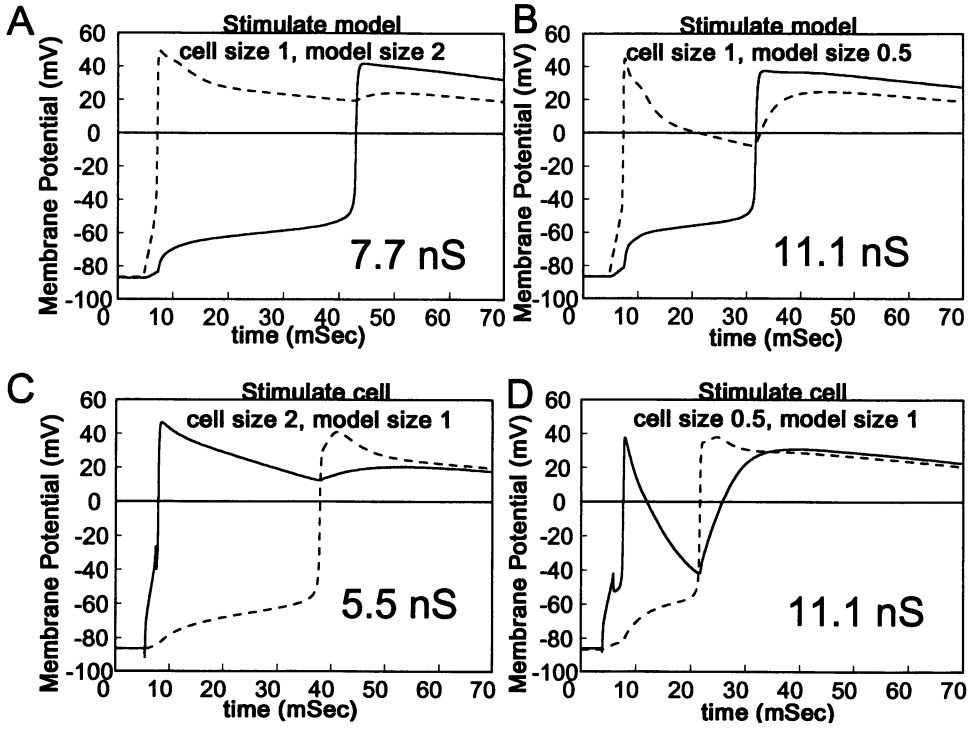

FIGURE 9 Effects of changing the size of the leader cell on conduction properties. *A* and *B* are plots comparing the action potential recorded from an isolated guinea pig ventricular cell (*solid line*) to the simultaneously produced LR model solution (*dotted line*) when the LR model was connected to the real cell by a conductance as indicated in the lower right corner of each panel that, for each panel, was the lowest coupling conductance for which conduction was successful. For *A* and *B* the periodic stimulus (1-Hz frequency) was applied to the LR model cell. For these two panels the LR model (leader cell) cell size has been adjusted to be either double that of the standard LR model cell (*A*) or half the size of the standard LR model cell (*B*) while the size of the real cell is adjusted to be equal to the standard LR model cell size, based on the determination of the current threshold for the real cell for a stimulus duration of 2 ms. *C* and *D* show the results when the periodic stimulus (1-Hz frequency) was applied to the real cell. For these two parts the real cell (leader cell) size has been adjusted to be either double that of the LR model cell (*C*) or half the size of the LR model cell (*D*), based on the determination of the current threshold for the real cell.

When we then continued to stimulate the model cell but halved the size of the model cell, we found (Fig. 9 *B*) that the required conductance was elevated to 11.1 nS and the early repolarization during the conduction process was increased. For 6 cells in which we applied this protocol, we found that the critical conductance for doubling the model cell size was 7.8 ± 0.6 nS and for halving the model cell size was 11.5 ± 1.2 nS. Both of these values were significantly different from the values obtained with equal cell size, being lower or greater, respectively. When we repeated this protocol with the real cell as the leader of the cell pair (Fig. 9, *C* and *D*) we obtained somewhat similar results. For doubling the size of the leader cell (the real cell) we found (Fig. 9 *C*) a critical conductance of 5.5 nS and the leader cell showed less early repolarization compared with the results obtained with stimulation of the real cell when the two cell sizes were the same (Fig. 7 *D*). When we then halved the size of the leader cell, we produced a very large early repolarization and increased the critical conductance to 11.1 nS. In 5 cells for which we applied this procedure, the critical conductance for stimulating the real cell while doubling the size of the real cell was 5.6 ± 0.2 nS while the critical conductance for halving the size of the real cell was 12.5 ± 1.4, each value significantly less or more, respectively, than the values obtained with stimulation of the real cell for equal cell size.

We summarize the results of Figs. 7–9 in Fig. 10 and in Table 1. We have also included simulation results in which we coupled two LR model cells to each other and found the critical coupling conductance under the same protocols of doubling or halving either the leader or the follower cell as we used experimentally. Looking first at these simulation results (labeled "Model to Model"), we see that the critical conductance for conduction when the size of the two cells is the same, is less for the LR model cell to LR model cell simulation than for either the conduction from real cell to LR model cell or conduction from LR model cell to real cell. Note that the horizontal axis for Fig. 10, *A* and *B* is "leader size/follower size." Because this parameter obviously can be adjusted by changing either the size of the leader or of the follower, we have divided our data into results obtained with changing the size of the follower cell (Fig. 10 *A*) and changing the size of the leader cell (Fig. 10 *B*). Note that the results for conduction from one LR model

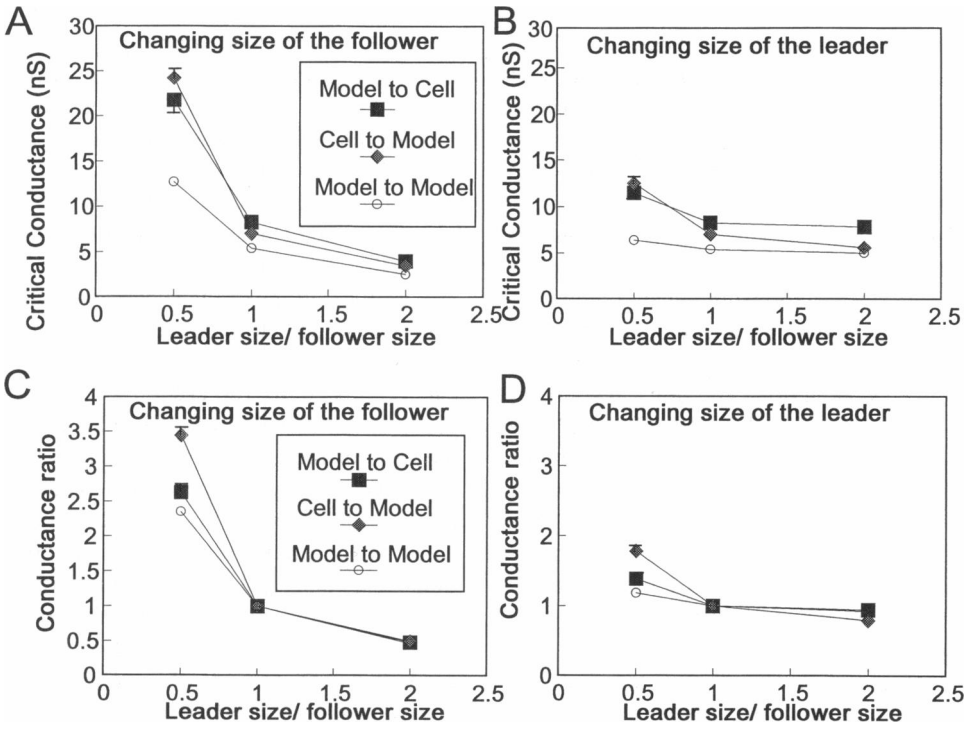

FIGURE 10 *A* and *B* show averaged results for a series of experiments in which the critical conductance for successful conduction was determined for real guinea pig ventricular cells coupled to the LR model cell simulation for which the recipient of the period stimulation was either the real cell (*diamonds*) or the LR model cell (*squares*). For *A*, the size of the "follower" was changed in a way such that size of the stimulated cell (real or LR model) was always set to the standard value for the LR model, based on the determination of the current threshold for a stimulus duration of 2 ms. The size of the non-stimulated cell (real or LR model) was then either doubled or halved to produce a ratio of leader size/follower size of either 0.5 or 2.0. For *B*, a similar procedure was used, except that the non-stimulated cell (real or LR model) remained at the standard size and the stimulated cell size was varied. Symbols are plotted as the mean values and the vertical lines indicate SEM when the value was larger than the size of the symbols. The corresponding results for simulated results when one LR model cell was connected to another LR model cell (*open circles*) are included for comparison. *C* and *D* are averaged results for the same series of experiments as for *A* and *B* when the critical conductance values have been normalized by the value obtained (for Model to Cell, Cell to Model, and Model to Model conduction) when conduction occurred between the two cells of equal sizes. Symbols are plotted as the mean values and the vertical lines indicate SEM when the value was larger than the size of the symbols.

cell to another LR model cell displays the same qualitative features that we have demonstrated experimentally here, with a significant increase in the required conductance when the follower size is increased and a significant decrease in the required conductance when the follower size is decreased (Fig. 10 *A*). Similarly, the results for conduction between two LR model cells also shows an effect of changing the size of the leader cell (Fig. 10 *B*), but it is clear that the magnitude of this effect is much smaller than the effects observed with changing the size of the follower. When we contrast the experimental data (either from real cell to LR model cell or from LR model cell to real cell) with the model cell to model cell data, we observe that all of the effects are occurring at somewhat higher critical conductances. Whereas the required conductance for real cell to model cell is less under conditions of equal size compared with the required conductance from model cell to real cell, there is an opposite relationship when the results are obtained under the condition of doubling the size of the follower cell (Fig. 10 *A*) or for halving the size of the leader cell (Fig. 10 *B*). The results become somewhat simpler if we emphasize only the geometrical changes by normalizing all of the critical conductances for each type of conduction (real cell to LR model, LR model to real cell, and LR model to LR model) to a standard value obtained when the sizes of the leader and the follower are equal, and these normalized results are expressed in Fig. 10, *C* and *D*, as values of "conductance ratio." There are now clearly demonstrated two different asymmetries in the relationships. For changes in the size of the follower cell (Fig. 10 *C*), the increases in the conductance ratio are much greater for increases in the follower size as compared to the decreases in the conductance ratio for decreases in the follower size. It is also clear that the differences in this relationship when comparing model cell to model cell conduction are less than the differences obtained with either model cell to real conduction or real cell to model cell conduction. The other asymmetry that is apparent is that, comparing Fig. 10, *C* and *D*, the effects of changing the size of the leader cell are much smaller than the effects of changing the size of the follower cell. For changing the size of the follower or changing the size of the leader, the results obtained when using conduction from the real cell to the model cell demonstrate the greatest effects of the leader size/follower size ratio on the critical conductance ratio.

As was clear from the data shown in Figs. 7–9 the maximal conduction delay was decreased when either the follower size was increased or the leader size was decreased. The data for all of the cells studied is summarized in Table 2 where we analyze the maximal conduction delay obtained under the conditions of LR model cell to LR model cell conduction, LR model cell to real cell conduction, and real cell to LR model cell conduction in the same format as for Table 1. For conduction from one LR model cell to another LR model cell the maximal conduction delays are somewhat longer than those we could experimentally obtain, and the effects of changing either the leader size or the follower size are less than those obtained experimentally with either the LR model cell or the real cell as the leader of the cell pair. For conduction delay, the results for increasing the size of the follower are exactly the same as for decreasing the size of the leader. Similarly, the results for decreasing the size of the follower are exactly the same as for increasing the size of the leader. It is clear that the maximal conduction delay depends only on the size ratio and not on the way in which it is changed. Very similar results were experimentally obtained. For conduction from the real cell to the LR model cell the changes in maximal conduction delay with changes in the leader or follower size were greater than for conduction from the LR model cell to the real cell. However, for both directions of conduction, the results for increasing the size of the follower were almost identical to those for decreasing the size of the leader, and the results for decreasing the size of the follower were almost identical to those for increasing the size of the leader.

DISCUSSION

Our results emphasize the interactions between the membrane properties of excitable cells, the geometrical factors of relative cell size, and the junctional conductance between cells to ultimately determine the success or failure of conduction. It is clear that all of these factors interact in even more complex ways when included within the complex and inhomogeneous distribution of cells of a cardiac syncytium. Nevertheless, we feel that it is useful to consider a simpler system in which these factors can be systematically varied and measured. The slow conduction and fractionated waveforms that are characteristic of conduction in infarcted tissue are indications of the successive activation of groups of cells for which the intergroup conductance is limiting the conduction. Our use of a model of two cells of variable sizes can be scaled to represent the conduction between two groups of cells under the conditions that, within each group, the cells of the group are themselves well coupled to each other and essentially isopotential. That this condition is met under certain conditions of myocardial infarction is indicated by the brief duration of each component of the fractionated signals, and also from direct microelectrode recordings of cells within the groups (Kienzle et al., 1987). Thus, the conduction between a group of 1000 cells connected by a conductance of 2500 nS to a group of 500 cells would have the same characteristics of electrical loading and also success or failure of conduction as one would observe between a single cell of twice the normal size connected to a cell of normal size by a conductance of 5 nS. In the case of the connections between large groups of cells, the interconnections might be a short bridge of cells, rather than a direct electrical connection between one cell of each group. Depending on the origin of the propagating action potential, the group of 1000 cells might serve as the leader or as the follower with respect to the group of 500 cells, and this represents the overall pathophysiological situation that we

are trying to understand. The major geometrical limitation of our model system is that, in intact tissue, each of the groups of cells is likely to be connected electrically to other groups of cells, but in our model system, we are currently restricted to a pair of cells without connections to other cells or groups of cells.

Although we have previously published results obtained with the coupling of two simultaneously recorded guinea pig ventricular cells (Sugiura and Joyner, 1992), we have used for this paper, an experimental setup with one real ventricular cell coupled to a real-time simulation of an isolated ventricular cell (the LR model cell). The advantage of this technique is that each of the real cells studied is coupled to an identical cell model, both as a leader and as a follower, so that we can systematically show the differences in the geometrical effects on electrical loading. The overall correspondence of the LR cell model with the recorded real cell action potentials is quite good. The strength-duration curves for the real cells and for the LR model cell are in general correspondence, but when the data for the real cells is normalized to that of the LR model cell for a stimulus duration of 2 ms, the excitability of the LR model cell is greater than for the real cell for longer stimulus durations, with about 30% less current required for stimulus durations of 10–20 ms. We summarize here the features we measured and the degree to which the LR cell model and the real cell correspond in their response to source and loading effects under conditions of extreme uncoupling: 1) When we normalized the real cell size to that of the LR model cell, we found that the required conductance for successful propagation was greater than that found for successful conduction between two LR model cells (5.4 nS), with a greater disparity (8.3 $\pm$ 0.6 nS) when we stimulated the LR model cell than that found (7.0 $\pm$ 0.2 nS) when we stimulated the real cell. 2) The extent of electrical loading of the action potentials, as indicated by the extent of the partial repolarization of the leader cell during the conduction process, was significantly greater for the real cell than for the LR model cell even when the size of the real cell was normalized to be equal to that of the LR model cell. 3) When the size of the follower cell was increased by a factor of two, the required conductance for successful conduction was dramatically increased; but this increase was greatest for the condition of conduction from a real cell to a LR model cell, less for conduction from the LR model cell to a real cell, and least for conduction from one LR model cell to another LR model cell. A similar discrepancy occurred when the size of the leader cell was decreased by a factor of two. 4) For all three conduction conditions (LR model cell to LR model cell, real cell to LR model cell, LR model cell to real cell) the effects on the required intercellular conductance of changes in the ratio of leader size to follower size were greater for changes in the follower size as compared to changes in the leader size and were also greater for interventions that reduced the ratio of leader size to follower size compared to interventions that increased the ratio of leader size to follower size. 5) For all three conduction conditions, the effects on the maximal conduction delay were an increase in the maximal conduction delay when the ratio of leader size to follower size was increased and a decrease in the maximal conduction delay when the ratio of leader size to follower size was decreased.

We emphasize that the model clamp technique, as we have used it in this work, is a test of the ability of the membrane model to accurately represent the properties of action potential conduction under conditions of extreme uncoupling. This technique does not test the applicability of the membrane model to represent specific ionic currents or changes in intracellular concentrations of ions since these are not being measured for the real cells in these experiments.

The conduction between two cardiac cells (or two groups of cardiac cells) can be considered to be determined by three components: 1) the intercellular conductance for intercellular current flow; 2) the amount of depolarization required in the follower cell to initiate an action potential (the "sink" for current flow); and 3) the ability of the leader cell to maintain a high membrane potential to serve as the "source" of current for the follower cell. During discontinuous conduction with long delays there are well documented abnormalities in the early plateau of the action potentials, recorded either from the Purkinje-ventricular junction (Tan et al., 1989) or from a pair of ventricular cells (Weingart and Maurer, 1988). We recently showed (Sugiura and Joyner, 1992) that, when two isolated guinea pig ventricular cells were coupled to each other by a variable conductance, the required intercellular conductance for successful conduction was increased by low doses of nifedipine, which specifically decreases the L-type calcium current (Kohlhardt and Fleckenstein, 1977). This effect was accompanied by a large increase in the extent of early repolarization of the leader cell and also by a decrease in the maximum delay for conduction. The present studies show similar effects of increasing the extent of repolarization, increasing the required intercellular conductance, and decreasing the maximum delay for conduction by decreasing the ratio of leader size to follower size. The relationship between these sets of results can be understood by considering the ability of the leader cell to supply current to the follower cell during the conduction process. It is clear that the L-type calcium current is a major ionic conductance, which tends to support the depolarization initiated by the sodium conductance during the early plateau. Therefore, either an intervention that decreases the inward current during this period (e.g., Nifedipine) or an intervention that increases the outward current during this period (e.g., electrical load imposed by a coupled cell) will have the effect of increasing the extent of early repolarization.

The current supplied by the leader cell during the conduction period is simply the difference in membrane potential between the leader cell and the follower cell multiplied by the intercellular conductance, whereas the current required for activation of the follower cell is determined primarily by the size of the follower cell. Thus, an increase in the size of the follower cell produces a demand for more

intercellular current flow during the conduction period. This can be accomplished by raising the intercellular conductance; and, if the electrical loading effects on the leader cell were not present (allowing the leader cell to have a constant ability to supply current), a doubling of the size of the follower cell would simply require a 100% increase of the intercellular conductance to produce twice the intercellular current flow. Similarly, in the absence of electrical loading effects on the leader cell, a halving of the size of the follower cell would allow conduction to occur with a 50% decrease of the previous intercellular conductance. From the same arguments, the maximum delay for conduction would be independent of the size of the follower cell if the electrical loading effects on the leader cell could be ignored. From the data of Table 1, it is clear that the electrical loading effects on the leader cell have a tremendous effect on the ability to conduct an action potential. When the follower size was doubled, the required intercellular conductance increased by 164% for conduction from the LR model cell to the real cell and 247% for conduction from the real cell to the LR model cell. Similarly, when the follower size was halved, the critical conductance decreased by 52% for conduction from the LR model to the real cell and by 59% for conduction from the real cell to the LR model cell. The influence of the geometrical factors on the maximum conduction delay is shown in Table 2. There is clearly a tremendous effect of the size ratio on maximum delay, with a doubling in the follower size decreasing the maximum delay by 35% for conduction from the LR model cell to the real cell and 47% for conduction from the real cell to the LR model cell. Halving the follower size increased the maximum delay 8% for conduction from the LR model cell to the real cell and 28% for conduction from the real cell to the LR model cell. Thus, the influence of the electrical load on the leader cell is very significant in determining not only the success or failure of conduction but also the maximum delay with which conduction can occur, with the real cell showing more electrical loading effects than the LR model cell. However, the geometrical factors are not the only factors that can determine success or failure of conduction. When the sizes of the leader and follower cell were the same, the conduction from the LR model cell to the real cell required greater conductance (8.3 nS) than for conduction from the real cell to the LR model cell (7.0 nS), which was still greater than that required for conduction from one LR model cell to another LR model cell (5.4 nS). This difference can be attributed to the greater excitability (requirement for a smaller stimulus current) for the LR model cell as compared to the real cell for long stimulus durations. The conductance required from one LR model cell to another LR model cell was the smallest value because of a combination of greater excitability of the follower cell and less electrical loading effects on the leader cell.

In summary, we have used the LR model cell coupled to a real guinea pig ventricular cell to investigate the effects of electrical loading on conduction delay, and the determinants of success or failure of conduction for a pair of cells. The phenomena we observed for the ventricular cell model were quantitatively different depending on whether the LR model cell or the real cell was used as the leader or follower. The differences between the LR model cell and the real cell in excitability and the susceptibility of the early plateau to repolarization with an imposed electrical load produce differences in action potential conduction that are explainable on the basis of a simple model of modulation of the ability of the leader cell to supply current. The differences between the real cells and the LR model cell in regard to action potential conduction appear to be primarily because of a greater susceptibility of real cells to electrical loading than that expressed by the LR model cell. Our results show that the actual anatomical features, including the size as well as the electrical interconnections of the surviving cell groups in a region of myocardial infarction may play a decisive role in the discontinuous conduction and conduction delays that occur within the infarct zone and differences in excitability may also play an important role.

This work was partially supported by National Institutes of Health grant HL22562 to Dr. Joyner, the Georgia Affiliate of the American Heart Association, the Emory Egleston Children's Research Center, Netherlands Heart Foundation grant 92.310, and Netherlands Organization for Scientific Research grant 805–06-152.

REFERENCES

Antzelevitch, C. and G. K. Moe. 1983. Electronic inhibitation and summation of impulse conduction in mammalian purkinje fibers. *Am. J. Physiol.* 245:H42–H53.

Beeler, G. W. and H. Reuter. 1977. Reconstruction of the action potential of ventricular myocardial fibres. *J. Physiol.* 268:177–210.

de Bakker, J. M., F. J. van Capelle, M. J. Janse, S. Tasseron, J. T. Vermeulen, N. de Jonge, and J. R. Lahpor. 1993. Slow conduction in the infarcted human heart. 'Zigzag' course of activation. *Circulation.* 88: 915–926.

De La Fuente, D., B. I. Sasnyiuk, and G. K. Moe. 1971. Conduction through a narrow isthmus in isolated canine atrial tissue. *Circulation.* 46:803–821.

Fenoglio, J. J., T. D. Pham, A. H. Harken, L. N. Horowitz, M. E. Josephson, and A. L. Wit. 1983. Recurrent sustained ventricular tachycardia: structure and ultrastructure of subendocardial regions in which tachycardia originates. *Circulation.* 68:518–533.

Gardner, P. I., P. C. Ursell, J. J. Fenoglio, and A. L. Wit. 1985. Electrophysiologic and anatomic basis for fractionated electrograms recorded from healed myocardial infarcts. *Circulation.* 72:596–611.

Hamill, O. P., A. Marty, E. Neher, B. Sakmann, and F. J. Sigworth. 1981. Improved patch-clamp techniques for high-resolution current recording from cells and cell-free membrane patches. *Pflueg. Arch. Euro. J. Physiol.* 391:85–100.

Joyner, R. W., H. Sugiura, and R. C. Tan. 1991. Unidirectional block between isolated rabbit ventricular cells coupled by a variable resistance. *Biophys. J.* 60:1038–1045.

Kienzle, M. G., R. C. Tan, B. M. Ramza, M. L. Young, and R. W. Joyner. 1987. Alterations in endocardial activation of the canine papillary muscle early and late after myocardial infarction. *Circulation.* 76:860–874.

Kohlhardt, M. and A. Fleckenstein. 1977. Inhibition of the slow inward current by nifedipine in mammalian ventricular myocardium. *Naunyn. Schmiedebergs. Arch. Pharmacol.* 298:267–272.

Kumar, R. and R. W. Joyner. 1994. An experimental model of the production of early afterdepolarizations by injury current from an ischemic region. *Pflueg. Arch. Euro. J. Physiol.* 428:425–432.

Luo, C. H. and Y. Rudy. 1991. A model of the ventricular cardiac action potential. Depolarization, repolarization, and their interaction. *Circ. Res.* 68:1501–1526.

Luo, C. H. and Y. Rudy. 1994a. A dynamic model of the cardiac ventricular action potential. I. Simulations of ionic currents and concentration changes. *Circ. Res.* 74:1071–1096.

Luo, C. H. and Y. Rudy. 1994b. A dynamic model of the cardiac ventricular action potential. II. After depolarizations, triggered activity, and potentiation. *Circ. Res.* 74:1097–1113.

Mendez, C., W. J. Mueller, J. Meredith, and G. K. Moe. 1969. Interaction of transmembrane potentials in canine purkinje fibers and at purkinje fiber-muscle junctions. *Circ. Res.* 24:361–373.

Spach, M. S., W. T. Miler, P. C. Dolber, J. M. Kootsey, J. R. Sommer, and C. E. Mosher. 1982. The functional role of structural complexities in the propagation of depolarization in the atrium of the dog. *Circ. Res.* 50:175–191.

Spear, J. F., E. L. Michelson, and E. N. Moore. 1983. Cellular electrophysiologic characteristics of chronically infarcted myocardium in dogs susceptible to sustained ventricular tachyarrhythmias. *J. Am. Coll. Cardiol.* 1:1099–1100.

Sugiura, H. and R. W. Joyner. 1992. Action potential conduction between guinea pig ventricular cells can be modulated by calcium current. *Am. J. Physiol.* 263:H1591–H1604.

Tan, R. C. and R. W. Joyner. 1990. Electrotonic influences on action potentials from isolated ventricular cells. *Circ. Res.* 67:1071–1081.

Tan, R. C., T. Osaka, and R. W. Joyner. 1991. Experimental model of effects on normal tissue of injury current from ischemic region. *Circ. Res.* 69:965–974.

Tan, R. C., B. M. Ramza, and R. W. Joyner. 1989. Modulation of the purkinje-ventricular muscle junctional conduction by elevated potassium and hypoxia. *Circulation.* 79:1100–1105.

Ursell, P. C., P. I. Gardner, A. Albala, J. J. Fenoglio, and A. L. Wit. 1985. Structural and electrophysiological changes in the epicardial border zone of canine myocardial infarcts during infarct healing. *Circ. Res.* 56: 436–451.

Veenstra, R. D., R. W. Joyner, and D. A. Rawling. 1984. Purkinje and ventricular activation sequences of canine papillary muscle. Effects of quinidine and calcium on the purkinje-ventricular conduction delay. *Circ. Res.* 54:500–515.

Victorri, B., A. Vinet, F. A. Roberge, and J. P. Drouhard. 1985. Numerical integration in the reconstruction of cardiac action potentials using Hodgkin-Huxley-type models. *Comput. Biomed. Res.* 18:10–23.

Weingart, R. and P. Maurer. 1988. Action potential transfer in cell pairs isolated from adult rat and guinea pig ventricles. *Circ. Res.* 63:72–80.